Mechanics of Advanced Composite Structures 8 (2021) 269 – 282

Semnan University

Mechanics of Advanced Composite Structures

journal homepage: http://MACS.journals.semnan.ac.ir

# Free Vibration Analysis of Combined Cylindrical-Conical Composite Shells using First-Order Shear Deformation Theory

**M. Soroush [a], A. Davar [a]*, J. Eskandari Jam [a], M. Heydari Beni [a], M. Eskandari Shahraki [b]**

[a] *Faculty of Materials and Manufacturing Processes, Malek Ashtar University of Technology, Iran.*
[b] *Department of Aerospace Engineering, Ferdowsi University of Mashhad, Mashhad, Iran*

**KEYWORDS**

Free vibration,
Cylindrical-conical composite shells,
First-order shear deformation theory

**ABSTRACT**

In this paper, a solution procedure is presented for free vibration of combined cylindrical-conical composite shells including the shear deformation effect of the shell. The solution presented in this study is obtained directly from the governing equations for five displacement components according to Hamilton's principle. This solution is in the form of a power series in terms of a particularly convenient coordinate system. In this study, the effects of geometry and material parameters on the natural frequencies are investigated. Also, to illustrate the validity of the present solution procedure, analytical results are verified with many studies and compared with those of the present numerical ABAQUS analysis. The outcomes showed a good agreement between the obtained results. The novelty of the present study is incorporating the transverse shear deformation in calculating the natural frequencies of the joined cylindrical-conical shells. In previous literature, this topic has not been studied in such a wide scope.

## 1. Introduction

Cylindrical and conical shells have widespread usage in the industry owing to their good mechanical and physical properties. Conical shells have not been as widely reported in the literature compared to cylindrical shells. This is due to the increased mathematical complexity associated with the effect of the variation of the radius along the length of the cone on the elastic waves. The approximate methods of calculating the natural frequencies for conical shells have been found by several authors [1], [2]. Many researchers, such as Love, Donnell-Mushtari, Timoshenko, Reissner, Flügge, and Sanders have presented various theories of shells with different assumptions and approximations for the sake of simplification. Many of them, such as Donnell-Mushtari, Timoshenko, Reissner, and Flügge have solved various shell problems based on Love's postulates [3]. He et al. studied a unified power series method for vibration analysis of composite laminate conical, a cylindrical shell, and an annular plate. They investigated the effect of the geometric parameters and material constants (e.g., elastic restrained spring stiffness constants, the angle between the shell surface and axis, length to the radius ratios, and modulus ratios) on the free vibration characteristics of the composite laminated structure [4] Kouchakzadeh and Shakouri studied the vibrational behavior of the two joined cross-ply laminated conical shells. They reviewed the natural frequency and effects of semi-vertex angles, meridional lengths, and shell thicknesses by solving the problem using Donnell theory and Hamilton's principle [5] Caresta and Kessissoglou offered a new recommendation based on Donnell-Mushtari and Flugge's equations to describe the free vibration characteristics of coupled isotropic cylindrical-conical shells. They also investigated the effects of the junction between the coupled shells and the boundary conditions [6]. Xianglong et al. studied the effects of the semi-vertex angle of the cone and the elastic restraint parameters on the free vibration behavior of the

* Corresponding author. Tel: (+98) 21-22936578
*E-mail address:* a_davar@mut.ac.ir

DOI: 10.22075/MACS.2021.20887.1278
Received 20-07-19; Received in revised form 21-01-17; Accepted 21-04-01

shell according to Reissner's thin shell theory [7]. Bagheri et al. evaluated the free vibration of joined conical-conical shells with higher-order shear deformation theory in various types of boundary conditions for the shell ends. The produced system of equations was discretized using the semi-analytical generalized differential quadrature (GDQ) method [8]. Mohammadrezazadeh and Jafari studied the nonlinear vibration analysis of laminated composite angle-ply cylindrical and conical shells. Also, they investigated the effects of several parameters including the layers' angle, the number of the layers, semi-vertex angle, length, and radius, as well as each layer's thickness on nonlinear frequency ratio, fundamental linear frequency [9]. Qin et al. studied a unified Fourier series solution for vibration analysis of FG-CNTRC cylindrical, conical shells, and annular plates with arbitrary boundary conditions. They used a micro-mechanical model based on the developed rule of mixtures [10]. Previously, no study has been conducted on the composite joined conical-cylindrical structures using first-order shear deformation theory (FSDT). In this research, the free vibration of joined conical-cylindrical composite shells is investigated based on higher-order shear deformation theory. After calculating the natural frequencies and verification of the results, the effect of geometric parameters material and lay-up is studied. The novelty of the present study is incorporating the transverse shear deformation in calculating the natural frequencies of the joined cylindrical-conical shells. In previous literature, this topic has not been studied in this wide scope.

## 2. Governing Equations for Joined Conical-Cylindrical Shells

Consider a joined conical-cylindrical shell made of a composite material of a uniform thickness of h, small radius of $R_1$, large (intersection) radius of $R_2$, slanted length of $L_c$, cylinder length of $L_s$, and vertex half angle of $\alpha$. Meridional, circumferential, and normal directions of the conical and cylindrical shell are denoted by $-\frac{L_c}{2} \le x_c \le \frac{L_c}{2}$, $-\frac{L_s}{2} \le x_s \le \frac{L_s}{2}$, $0 \le \theta \le 2\pi$, and $-\frac{h}{2} \le z \le +\frac{h}{2}$, respectively. The adopted coordinates system $(x_c,\theta_c,z_c,x_s,\theta_s,z_s)$, geometric characteristics, and sign convention of the joined shell are depicted in Fig. 1. Also, displacement components for the cone and cylinder in coordinate system directions are $(u_c,v_c,w_c)$ and $(u_s,v_s,w_s)$, respectively.

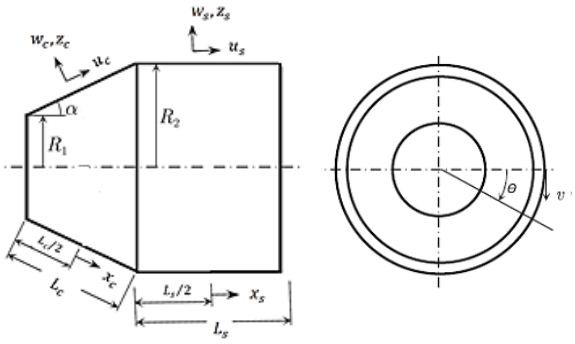


**Fig. 1**. Schematic of a thin joined cylindrical-conical shell

To capture the thickness shear deformations and rotary inertia effects of the conical-cylindrical shell, FSDT was used to formulate the governing equations of the shell. Based on FSDT, components of the displacement on a generic point are represented according to the mid-surface characteristics as follows:

For conical shell:

$$u_c(x,\theta,z,t) = u_{0c}(x,\theta,t) + z\emptyset_{xc}(x,\theta,t) \quad (1)$$

$$v_c(x,\theta,z,t) = v_{0c}(x,\theta,t) + z\emptyset_{\theta c}(x,\theta,t) \quad (2)$$

$$w_c(x,\theta,z,t) = w_{0c}(x,\theta,t) \quad (3)$$

For cylindrical shell:

$$u_s(x,\theta,z,t) = u_{0s}(x,\theta,t) + z\emptyset_{xs}(x,\theta,t) \quad (4)$$

$$v_s(x,\theta,z,t) = v_{0s}(x,\theta,t) + z\emptyset_{\theta s}(x,\theta,t) \quad (5)$$

$$w_s(x,\theta,z,t) = w_{0s}(x,\theta,t) \quad (6)$$

In the above equations, $u_c$, $v_c$, and $w_c$ are the meridional, circumferential, and normal displacements of the conical shell, respectively. Also, $u_s$, $v_s$, and $w_s$ are the radial, circumferential, and normal displacements of the cylindrical shell, respectively

A subscript 0 denotes the characteristics of the mid-surface. Besides, $\emptyset_{xc}$ , $\emptyset_{\theta c}$ , $\emptyset_{xs}$, and $\emptyset_{\theta s}$ are the transverse normal rotations about the $x$ and $\theta$ axes for conical and cylindrical shells, respectively. According to FSDT, the components of the strain field on an arbitrary point of the conical and cylindrical are be obtained in terms of strains and curvatures of the mid-surface of the shell as follows:

For conical shell:

$$\begin{bmatrix} \varepsilon_{xx,c} \\ \varepsilon_{\theta\theta,c} \\ \gamma_{x\theta,c} \\ \gamma_{xz,c} \\ \gamma_{\theta z,c} \end{bmatrix} = \begin{bmatrix} \dot{\varepsilon}_{xx,c} \\ \dot{\varepsilon}_{\theta\theta,c} \\ \dot{\gamma}_{x\theta,c} \\ \dot{\gamma}_{xz,c} \\ \dot{\gamma}_{\theta z,c} \end{bmatrix} + z \begin{bmatrix} \kappa_{xx,c} \\ \kappa_{\theta\theta,c} \\ \kappa_{x\theta,c} \\ \kappa_{xz,c} \\ \kappa_{\theta z,c} \end{bmatrix} \quad (7)$$

For cylindrical shell:

$$\begin{bmatrix}\varepsilon_{xx,s}\\ \varepsilon_{\theta\theta,s}\\ \gamma_{x\theta,s}\\ \gamma_{xz,s}\\ \gamma_{\theta z,s}\end{bmatrix}=\begin{bmatrix}\dot{\varepsilon}_{xx,s}\\ \dot{\varepsilon}_{\theta\theta,s}\\ \dot{\gamma}_{x\theta,s}\\ \dot{\gamma}_{xz,s}\\ \dot{\gamma}_{\theta z,s}\end{bmatrix}+z\begin{bmatrix}\kappa_{xx,s}\\ \kappa_{\theta\theta,s}\\ \kappa_{x\theta,s}\\ \kappa_{xz,s}\\ \kappa_{\theta z,s}\end{bmatrix} \tag{8}$$

According to Love's theory, the kinematic relations between the displacement components and strain and curvatures are [13]:

$$\dot{\varepsilon}_{xx}=\frac{\partial u_0}{\partial x} \tag{9}$$

$$\dot{\varepsilon}_{\theta\theta}=\frac{1}{R(x)}\left(\frac{\partial v_0}{\partial\theta}+u_0 sin\alpha+w_0 cos\alpha\right) \tag{10}$$

$$\dot{\gamma}_{x\theta}=\frac{1}{R(x)}\frac{\partial u_0}{\partial\theta}-\frac{1}{R(x)}v_0 sin\alpha+\frac{\partial v_0}{\partial x} \tag{11}$$

$$\dot{\gamma}_{xz}=\frac{\partial w_0}{\partial x}+\emptyset_x \tag{12}$$

$$\dot{\gamma}_{\theta z}=\frac{1}{R(x)}\frac{\partial w_0}{\partial\theta}+\emptyset_\theta-\frac{v_0 cos\alpha}{R(x)} \tag{13}$$

$$k_{xx}=\frac{\partial\emptyset_x}{\partial x} \tag{14}$$

$$k_{\theta\theta}=\frac{1}{R(x)}(\emptyset_x sin\alpha+\frac{\partial\emptyset_\theta}{\partial\theta}) \tag{15}$$

$$k_{x\theta}=\frac{1}{R(x)}\frac{\partial\emptyset_x}{\partial\theta}+\frac{\partial\emptyset_\theta}{\partial x}-\frac{1}{R(x)}\emptyset_\theta sin\alpha \tag{16}$$

In the above equations, $\alpha$ is the angle of the semi-vertex of the conical shell. In the case of a cylindrical shell, $\alpha$ is equal to 0 and $(x)=R_2$ .

In Eqs. (9) to (16), in case of a conical shell, $\emptyset_x=\emptyset_{xc}$ , $\emptyset_\theta=\emptyset_{\theta c}$ , $u_0=u_{0c}$ , $v_0=v_{0c}$ , and $w_0=w_{0c}$. Also, in the case of a cylindrical shell, $\emptyset_x=\emptyset_{xs}$ , $\emptyset_\theta=\emptyset_{\theta s}$ , $u_0=u_{0s}$ , $v_0=v_{0s}$, and $w_0=w_{0s}$.

The dynamic version of the principle of virtual work (Hamilton's principle) is expressed as follows [10]:

$$\int_0^T(\delta k_i-\delta U_i)dt=0 \quad i=c,s \tag{17}$$

where $\delta U_i$ denotes the virtual strain energy, $\delta V_i$ is the virtual potential energy due to the applied loads, and $\delta k_i$ shows the virtual kinetic energy.

$$\begin{aligned}k_i=&\iiint_{V_i}\rho_i(\dot{u}_\iota\delta\dot{u}_i+\dot{v}_\iota\delta\dot{v}_i+\\ &\dot{w}_i\delta\dot{w}_\iota)dV_i=\iint_{A_i}\int_{-\frac{h}{2}}^{\frac{h}{2}}\{I_{0,i}\big(\dot{u}_{0,i}\delta\dot{u}_{0,i}+\\ &\dot{v}_{0,i}\delta\dot{v}_{0,i}+\dot{w}_{0,i}\delta\dot{w}_{0,i}\big)+I_{1,i}\big(\dot{u}_{0,i}\delta\dot{\emptyset}_{x,i}+\\ &\dot{\emptyset}_{x,i}\delta\dot{u}_{0,i}+\dot{v}_{0,i}\delta\dot{\emptyset}_{\theta,i}+\dot{\emptyset}_{\theta,i}\delta\dot{v}_{0,i}\big)+\\ &I_{2,i}\big(\dot{\emptyset}_{x,i}\delta\dot{\emptyset}_{x,i}+\dot{\emptyset}_{\theta,i}\delta\dot{\emptyset}_{\theta,i}\big)\}R_i(x)dx_i d\theta_i\end{aligned} \tag{18}$$

$$\begin{aligned}U_i=&\iint_{A_i}(N_{11,i}\delta\dot{\varepsilon}_{11,i}+N_{22,i}\delta\dot{\varepsilon}_{22,i}+\\ &N_{12,i}\delta\dot{\varepsilon}_{12,i}+N_{21,i}\delta\dot{\varepsilon}_{21,i}+M_{11,i}\delta k_{x,i}+\\ &M_{22,i}\delta k_{y,i}+M_{12,i}\delta k_{xy,i}+\\ &M_{21,i}\delta k_{xy,i}+Q_{x,i}\delta\dot{\varepsilon}_{13,i}+\\ &Q_{\theta,i}\delta\dot{\varepsilon}_{23,i})R_i(x)dx_i d\theta_i\end{aligned} \tag{19}$$

where [11]

$$I_i=\int_{-\frac{h}{2}}^{\frac{h}{2}}\rho\, z^i dz \quad i=1,2,3 \tag{20}$$

where ρ is the density of shell material.

The relation between the stress resultants and stress fields is:

For the conical shell:

$$\begin{bmatrix}N_{11,c}\\ N_{22,c}\\ N_{12,c}\\ N_{21,c}\\ M_{11,c}\\ M_{22,c}\\ M_{12,c}\\ M_{21,c}\end{bmatrix}=\int_{-\frac{h}{2}}^{\frac{h}{2}}\begin{bmatrix}\sigma_{11,c}\\ \sigma_{22,c}\\ \sigma_{12,c}\\ \sigma_{21,c}\\ z\sigma_{11,c}\\ z\sigma_{22,c}\\ z\sigma_{12,c}\\ z\sigma_{21,c}\end{bmatrix}dz \tag{21}$$

$$\begin{bmatrix}Q_{1,c}\\ Q_{2,c}\end{bmatrix}=\int_{-\frac{h}{2}}^{\frac{h}{2}}\begin{bmatrix}\sigma_{13,c}\\ \sigma_{23,c}\end{bmatrix}dz \tag{22}$$

For the cylindrical shell:

$$\begin{bmatrix}N_{11,s}\\ N_{22,s}\\ N_{12,s}\\ N_{21,s}\\ M_{11,s}\\ M_{22,s}\\ M_{12,s}\\ M_{21,s}\end{bmatrix}=\int_{-\frac{h}{2}}^{\frac{h}{2}}\begin{bmatrix}\sigma_{11,s}\\ \sigma_{22,s}\\ \sigma_{12,s}\\ \sigma_{21,s}\\ z\sigma_{11,s}\\ z\sigma_{22,s}\\ z\sigma_{12,s}\\ z\sigma_{21,s}\end{bmatrix}dz \tag{23}$$

$$\begin{bmatrix}Q_{1,s}\\ Q_{2,s}\end{bmatrix}=\int_{-\frac{h}{2}}^{\frac{h}{2}}\begin{bmatrix}\sigma_{13,s}\\ \sigma_{23,s}\end{bmatrix}dz \tag{24}$$

where $(N_{11}, N_{22}, N_{12})$ and $(M_{11}, M_{22}, M_{12})$ are stress and moment resultants per unit length, respectively. Moreover, $\sigma_{ij}$ shows the elements of the stress vector, defined in [11].

## 3. Equilibrium Equations

After substituting the above relations in Eq. (17), and partial integration and collecting similar terms, governing equations for the equilibrium of the conical shell are obtained as follows:

$$\frac{\partial N_{11}}{\partial x}+(N_{11}-N_{22})\frac{\sin\alpha}{R(x)}+\frac{\partial N_{12}}{R(x)\partial\theta}-q_l+P\left(\frac{\partial^2 u}{R(x)\partial\theta^2}\right)=I_0\ddot{u}_0+I_1\ddot{\emptyset}_1 \quad (25)$$

$$\frac{\partial N_{22}}{R(x)\partial\theta}+2(N_{12})\frac{\sin\alpha}{R(x)}+\frac{\partial N_{12}}{\partial x}+\frac{Q_2\cos\alpha}{R(x)}-q_\theta+P\left(\frac{\partial^2 v}{R(x)\partial\theta^2}\right)=I_0\ddot{v}_0+I_1\ddot{\emptyset}_2 \quad (26)$$

$$-\frac{N_{22}\cos\alpha}{R(x)}+\frac{\partial Q_1}{\partial x}+\frac{Q_1\sin\alpha}{R(x)}+\frac{\partial Q_2}{R(x)\partial\theta}-q_r+P\left(\frac{\partial^2 w}{R(x)\partial\theta^2}\right)+N_a\frac{\partial^2 w}{\partial x^2}=I_0\ddot{w}_0 \quad (27)$$

$$\frac{\partial M_{11}}{\partial x}+(M_{11}-M_{22})\frac{\sin\alpha}{R(x)}+\frac{\partial M_{12}}{R(x)\partial\theta}-Q_1=I_1\ddot{u}_0+I_2\ddot{\emptyset}_1 \quad (28)$$

$$\frac{\partial M_{22}}{R(x)\partial\theta}+2(M_{12})\frac{\sin\alpha}{R(x)}+\frac{\partial M_{12}}{\partial x}-Q_2=I_1\ddot{v}_0+I_2\ddot{\emptyset}_2 \quad (29)$$

In the above equations, $P$ is internal pressure and $N_a$ is axial force. For cylindrical shells, $R(x)=R_2$ and $\alpha$ is set to be equal to 0.

## 4. Constitutive Equations

The constitutive relations for the laminated conical-cylindrical shell are expressed as follows:

$$\begin{bmatrix}N_{11}\\N_{22}\\N_{12}\\M_{11}\\M_{22}\\M_{12}\end{bmatrix}=\begin{bmatrix}A_{11}&A_{12}&A_{16}&B_{11}&B_{12}&B_{16}\\A_{21}&A_{22}&A_{26}&B_{21}&B_{22}&B_{26}\\A_{61}&A_{62}&A_{66}&B_{61}&B_{62}&B_{66}\\B_{11}&B_{12}&B_{16}&D_{11}&D_{12}&D_{16}\\B_{21}&B_{22}&B_{26}&D_{21}&D_{22}&D_{26}\\B_{61}&B_{62}&B_{66}&D_{61}&D_{62}&D_{66}\end{bmatrix}\begin{bmatrix}\dot{\varepsilon}_{11}\\\dot{\varepsilon}_{22}\\\dot{\varepsilon}_{12}\\k_1\\k_2\\k_{12}\end{bmatrix} \quad (30)$$

$$\begin{bmatrix}Q_2\\Q_1\end{bmatrix}=k_s\begin{bmatrix}A_{44}&A_{45}\\A_{54}&A_{55}\end{bmatrix}\begin{bmatrix}\dot{\varepsilon}_{23}\\\dot{\varepsilon}_{13}\end{bmatrix} \quad (31)$$

where $k_s$ is the shear correction factor and is considered to be equal to $\pi^2/12$ according to Mindlin's assumptions [11]. Also, $A_{ij}$ , $B_{ij}$, and $D_{ij}$ are composite stiffness matrices defined in [12].

## 5. Boundary Conditions

All types of boundary conditions can be used at both ends of the cone or the cylinder. The simply supported boundary conditions at $x_c=-L_c/2$ and $x_s=+L_s/2$ are expressed as follows:

$$v=w=\emptyset_2=N_x=M_x=0 \quad (32)$$

## 6. Continuity Conditions

The continuity conditions at the joint of the two shells can be represented as follows:

$$at\ x_c=L_c/2\ \ \&\ x_s=-L_s/2:$$

$$u_c\cos\alpha-w_c\sin\alpha=u_s \quad (33)$$

$$u_c\sin\alpha+w_c\cos\alpha=w_s \quad (34)$$

$$v_c=v_s \quad (35)$$

$$\emptyset_{1c}=\emptyset_{1s} \quad (36)$$

$$\emptyset_{2c}=\emptyset_{2s} \quad (37)$$

$$N_{xc}\cos\alpha-Q_{xc}\sin\alpha=N_{xs} \quad (38)$$

$$N_{xc}\sin\alpha+Q_{xc}\cos\alpha=Q_{xs} \quad (39)$$

$$N_{x\theta_c}=N_{x\theta_s} \quad (40)$$

$$M_{xc}=M_{xs} \quad (41)$$

$$M_{x\theta c}=M_{x\theta s} \quad (42)$$

For solving the above equations, solutions of the following form are assumed such that they exactly satisfy both the boundary and the continuity conditions:

For the conical shell:

$$u_{0,c}(x,\theta,t)=U_c(x)\cos n\theta\ e^{-j\omega t} \quad (39)$$

$$v_{0,c}(x,\theta,t)=V_c(x)\sin n\theta\ e^{-j\omega t} \quad (40)$$

$$w_{0,c}(x,\theta,t)=W_c(x)\cos n\theta\ e^{-j\omega t} \quad (41)$$

$$\emptyset_{x,c}(x,\theta,t)=\Phi_{x,c}(x)\cos n\theta\ e^{-j\omega t} \quad (42)$$

$$\emptyset_{\theta,c}(x,\theta,t)=\Phi_{\theta,c}(x)\sin n\theta\ e^{-j\omega t} \quad (43)$$

For the cylindrical shell:

$$u_{0,s}(x,\theta,t) = U_s(x)\cos n\theta\, e^{-j\omega t} \quad (44)$$

$$v_{0,s}(x,\theta,t) = V_s(x)\sin n\theta\, e^{-j\omega t} \quad (45)$$

$$w_{0,s}(x,\theta,t) = W_s(x)\cos n\theta\, e^{-j\omega t} \quad (46)$$

$$\emptyset_{x,s}(x,\theta,t) = \Phi_{x,s}(x)\cos n\theta\, e^{-j\omega t} \quad (47)$$

$$\emptyset_{\theta,s}(x,\theta,t) = \Phi_{\theta,s}(x)\sin n\theta\, e^{-j\omega t} \quad (48)$$

where

$$U_i(x) = \sum_{m=0}^{\infty} a_{m,i}{x_i}^m \;\; i = c,s \quad (49)$$

$$V_i(x) = \sum_{m=0}^{\infty} b_{m,i}{x_i}^m \; i = c,s \quad (50)$$

$$W_i(x) = \sum_{m=0}^{\infty} c_{m,i}{x_i}^m \;\; i = c,s \quad (51)$$

$$\Phi_{x,i}(x) = \sum_{m=0}^{\infty} d_{m,i}{x_i}^m \; i = c,s \quad (52)$$

$$\Phi_{\theta,i}(x) = \sum_{m=0}^{\infty} f_{m,i}{x_i}^m \;\; i = c,s \quad (53)$$

After substituting the above functions in the governing Eqs. (25) to (29), the following recurrence relations are obtained:

$$\begin{aligned} a_{m+2} = {} & T_{11}a_{m+1} + T_{12}a_m + T_{13}a_{m-1} \\ & + T_{14}a_{m-2} + T_{15}b_{m+1} + T_{16}b_m \\ & + T_{17}c_{m+1} + T_{1,8}c_m + T_{1,9}c_{m-1} \\ & + T_{1,10}d_{m+1} + T_{1,11}d_m + T_{1,12}d_{m-1} \\ & + T_{1,13}d_{m-2} + T_{1,14}f_{m+1} + T_{1,15}f_m \end{aligned} \quad (54)$$

$$\begin{aligned} b_{m+2} = {} & T_{21}a_{m+1} + T_{22}a_m + T_{23}b_{m+1} \\ & + T_{24}b_m + T_{25}b_{m-1} + T_{26}b_{m-2} \\ & + T_{2,7}c_m + T_{2,8}c_{m-1} + T_{2,9}d_{m+1} \\ & + T_{2,10}d_m + T_{2,11}f_{m+1} + T_{2,12}f_m \\ & + T_{2,13}f_{m-1} + T_{2,14}f_{m-2} \end{aligned} \quad (55)$$

$$\begin{aligned} c_{m+2} = {} & T_{31}a_{m+1} + T_{32}a_m + T_{33}b_m \\ & + T_{34}c_{m+1} + T_{3,5}c_m + T_{3,6}c_{m-1} \\ & + T_{3,7}c_{m-2} + T_{3,8}d_{m+1} + T_{3,9}d_m \\ & + T_{3,10}d_{m-1} + T_{3,11}f_m + T_{3,12}f_{m-1} \end{aligned} \quad (56)$$

$$\begin{aligned} d_{m+2} = {} & T_{41}a_{m+1} + T_{42}a_m + T_{43}a_{m-1} \\ & + T_{44}a_{m-2} + T_{45}b_{m+1} + T_{46}b_m \\ & + T_{47}c_{m+1} + T_{4,8}c_m + T_{4,9}c_{m-1} \\ & + T_{4,10}d_{m+1} + T_{4,11}d_m + T_{4,12}d_{m-1} \\ & + T_{4,13}d_{m-2} + T_{4,14}f_{m+1} + T_{4,15}f_m \end{aligned} \quad (57)$$

$$\begin{aligned} f_{m+2} = {} & T_{51}a_{m+1} + T_{52}a_m + T_{53}b_{m+1} \\ & + T_{54}b_m + T_{55}b_{m-1} + T_{56}b_{m-2} \\ & + T_{5,7}c_m + T_{5,8}c_{m-1} + T_{5,9}d_{m+1} \\ & + T_{5,10}d_m + T_{5,11}f_{m+1} + T_{5,12}f_m \\ & + T_{5,13}f_{m-1} + T_{5,14}f_{m-2} \end{aligned} \quad (58)$$

where $T_{ij}$ parameters are introduced in the Appendix.

After applying the continuity and boundary conditions and global assembling, a general relation is obtained as follows:

$$KX - [M_1\omega^2 + M_2\omega^4 + \cdots]X = [0] \quad (59)$$

where M is the generalized mass matrix, K is the generalized stiffness matrix, and X is the unknown displacement vector (mode shape). The natural frequencies of the structure are obtained by solving the above equation using numerical techniques within a MATLAB code.

## 7. Numerical Results and Discussion

Finite element modeling (FEM) was performed in ABAQUS 13.6 software. The geometric model made in the software is a shell model. A total of 13,460 S4R shell elements were used for meshing. The procedure described in the previous sections is used herein to study the free vibration of joined conical-cylindrical shell system made of composite material. In this section, first, some comparison studies are conducted. Next, parametric studies are performed to examine the influences of involved parameters. Numerical calculations show that including 50 terms ($m$=50) in the series solution provides satisfactorily converged results for the natural frequencies. The element type is quadratic 8-node shell element (S8R). The number of elements increases from 4500 up to 520000 elements. When the number of elements reaches 94,000, the results started to converge (Fig. 2).

Before presenting the results, the non-dimensional frequency parameter is introduced as follows:

$$\omega_c = \sqrt{\frac{\rho h}{A_{11}}}\,\omega R_2 \quad (60)$$

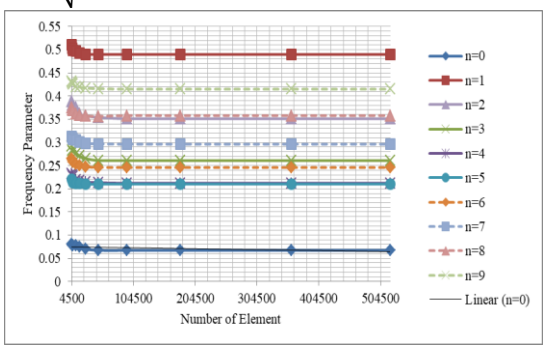


**Fig. 2.** The convergence of the frequency parameter $\omega_c$ for a simply supported - simply supported joined isotropic conical–cylindrical shell based on element number

## 8. Comparison Studies

The first comparison study calculates the first six frequencies of a joined cylindrical-conical shell for each circumferential mode number n. The numerical results of this study are compared with those reported in several references as shown in Table 1.

For an isotropic combined conical-cylindrical shell, the material and geometric parameters are:

$E = 211\ GPa\ ,\ \ \nu = 0.3\ , \rho = 7800\frac{kg}{m^3}$

$\frac{L_s}{R_s} = 0.5\ , h = 0.01R_s\ , R_c = 0.4226R_s\ , \alpha = 30°$

where $\omega$ and $\omega_c$ are referred to as the frequency and its parameter of the combined shell.

The frequency parameters were compared for a combined shell with the above materials, geometric parameters, and simply-supported boundary conditions at both ends with ABAQUS. The model is shown in Fig. 3.

The results are shown in Table 2.

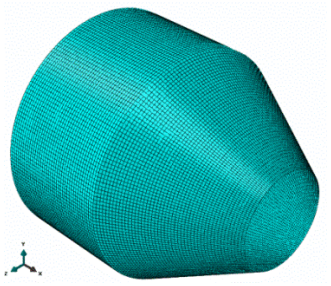

(a)

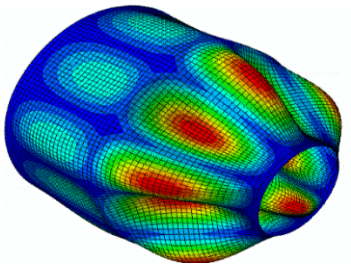

(b)

**Fig. 3**. Finite element model in ABAQUS: a) Elements mesh pattern and b) Lowest asymmetric shape ($n$=5)

**Table 1**. Comparison of dimensionless frequency parameter ω_c for a free-clamped joined isotropic conical-cylindrical shell

| $n$ | $\omega_c$ | | | | |
|---|---|---|---|---|---|
| | Present | Kouchakzadeh and Shakouri [5] | Caresta and Kessissoglou [6] | Efraim and Eisenberger [11] | Irie et al. [4] |
| 0 | 0.5035 | 0.5038 | 0.5038 | 0.5038 | 0.5047 |
| 1 | 0.2928 | 0.2929 | 0.2929 | 0.2929 | 0.2930 |
| 2 | 0.1103 | 0.1000 | 0.1020 | 0.1000 | 0.1010 |
| 3 | 0.0952 | 0.0876 | 0.09377 | 0.0876 | 0.9076 |
| 4 | 0.1512 | 0.1446 | 0.1506 | 0.1446 | 0.1477 |
| 5 | 0.1986 | 0.1995 | 0.2039 | 0.1995 | 0.2021 |

**Table 2**. Comparison of the dimensionless frequency parameter $\omega_c$ for a simply supported joined isotropic conical-cylindrical shell

| $n$ | $\omega_c$ | | |
|---|---|---|---|
| | Present (Analytical) | Present (ABAQUS) | Error Percents |
| 0 | 0.0651 | 0.067 | 2.91% |
| 1 | 0.4925 | 0.4898 | 0.27% |
| 2 | 0.3509 | 0.3512 | 0.03% |
| 3 | 0.2597 | 0.2609 | 0.12% |
| 4 | 0.2117 | 0.2121 | 0.04% |
| 5 | 0.2121 | 0.2102 | 0.19% |
| 6 | 0.2448 | 0.2458 | 0.1% |
| 7 | 0.2944 | 0.2963 | 0.19% |
| 8 | 0.3512 | 0.3580 | 0.68% |
| 9 | 0.4136 | 0.4150 | 0.14% |

According to Table 2, the fundamental frequency occurs at $n$=4 (for analytical method) and $n$=5 (for the ABAQUS method), indicating a close agreement.

## 9. Parametric Studies

After validating the proposed solution method, we analyzed the results of the natural frequencies for the free vibration of a shear deformable conical-cylindrical shell system made of a linearly elastic composite material. In this section, the composite cylindrical-conical shell with E-glass epoxy properties (Table 3) and geometrical properties (Table 4) is investigated. The considered lay-up is [0/90]. Unless stated otherwise, the properties mentioned in Tables 3 and 4 were applied. The boundary condition is simply supported at two ends.

## 10. Effect of the Cone Semi-vertex Angle

The effect of the semi-vertex angle of the composite cylindrical-conical shell on the natural frequencies is investigated in Figs. 4 to 6.

**Table 3**. Properties of the material of composite shell [14], [15]

| Material | $\rho$ $(\frac{kg}{m^3})$ | $E_1$ $(GPa)$ | $E_2$ $(GPa)$ | $G_{12}$ $(GPa)$ | $\upsilon_{12}$ |
|---|---|---|---|---|---|
| E-Glass/Epoxy | 2100 | 39.2 | 8.6 | 3.7 | 0.28 |

**Table 4**. Geometric parameters of the conical shell

| $L_c = L_s$ $(mm)$ | $R_s(mm)$ | $R_c(mm)$ | $h(mm)$ | Composite lay-up angles |
|---|---|---|---|---|
| 200 | $l_s$ | $0.4226R_s$ | $0.01R_s$ | [0 / 90] |

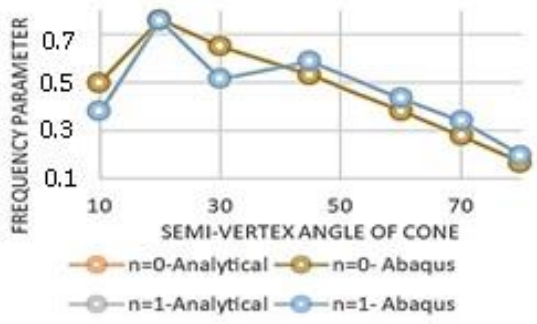


**Fig. 4**. Natural frequency parameter versus semi-vertex angle of the cone for circumferential wave numbers ($n$=0,1)

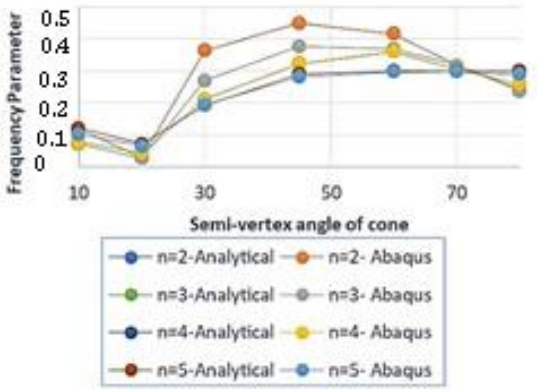


**Fig. 5**. Natural frequency parameter versus semi-vertex angle of the cone for circumferential wave numbers ($n$=2:5)

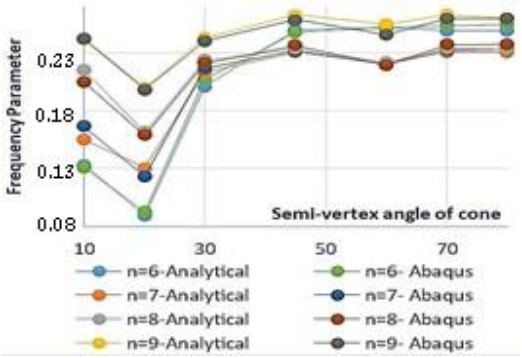


**Fig. 6**. Natural frequency parameter versus semi vertex angle of the cone for circumferential wave numbers ($n$=6:9)

As can be seen from Figs. 4 to 6, by increasing the semi-vertex angle of the cone, for higher values of the circumferential wave number ($n$=6:9), the natural frequency is converged to an almost constant value. Also, the minimum natural frequency for the values of n greater than 1 occurs at $\alpha = 20°$ while the maximum natural frequency occurs at $\alpha = 20°$ for $n$=0 and $n$=1. For $n$=0, by increasing the semi-vertex angle, the natural frequency is first increased and then decreased. However, for other values of n, no special trend exists. Just for higher values on n ($n$=6:9), the natural frequency is converged to a special value for higher values of.

## 11. Effect of Thickness

The effect of the thickness of the shell on the natural frequency is represented in Table 5

As can be seen in Table 5, by increasing the value of $h/R_2$ from 0.01 to 0.03, the fundamental mode number (n) is decreased. However, it is unchanged by increasing the value of $h/R_2$ from 0.03 to 0.05 ($n$=3).

## 12. Effect of Length of Shell

The effect of the length ratio of the combined shell on the natural frequency is studied in Fig. 7. The radius of the cylindrical shell is assumed to be constant. Also, for a specific value of the $\frac{L_s}{R_s}$ ratio, the ratio of $\frac{L_s}{L_c}$ is changed by changing the value of $L_c$ . The lay-up of the composite shell is considered to be $[0 / 90]_2$.

**Table 5**. Effect of thickness of the shell on the frequency parameter of a conical-cylindrical composite shell

| $h/R_2$ | n | | | | | |
|---|---|---|---|---|---|---|
| | 0 | 1 | 2 | 3 | 4 | 5 |
| 0.01 | 0.663 | 0.534 | 0.371 | 0.261 | 0.220 | 0.191* |
| 0.02 | 0.715 | 0.562 | 0.399 | 0.310 | 0.270* | 0.295 |
| 0.03 | 0.756 | 0.584 | 0.410 | 0.321* | 0.333 | 0.368 |
| 0.04 | 0.772 | 0.606 | 0.424 | 0.359* | 0.391 | 0.436 |
| 0.05 | 0.781 | 0.611 | 0.421 | 0.378* | 0.438 | 0.491 |

*: Lowest (fundamental) mode number

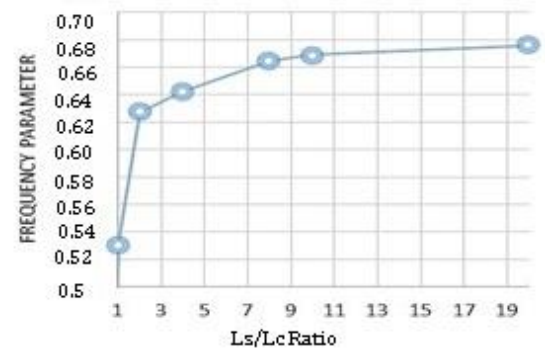


(a)

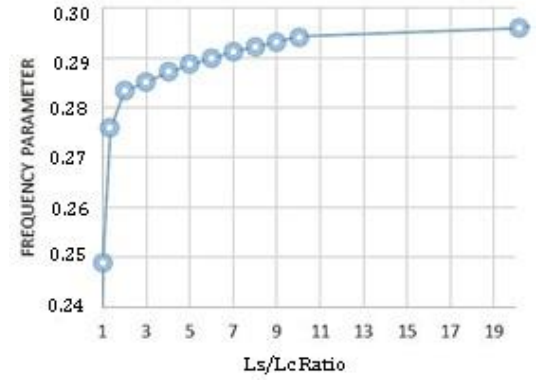


(b)

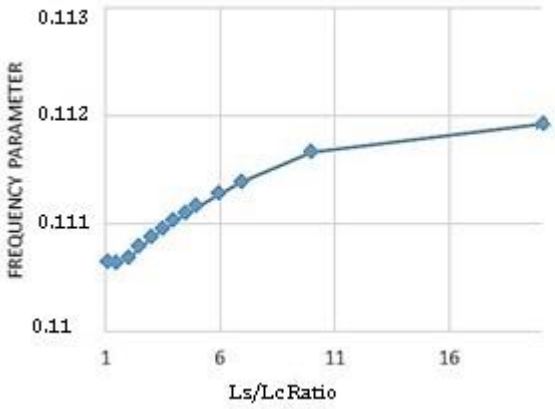


(c)

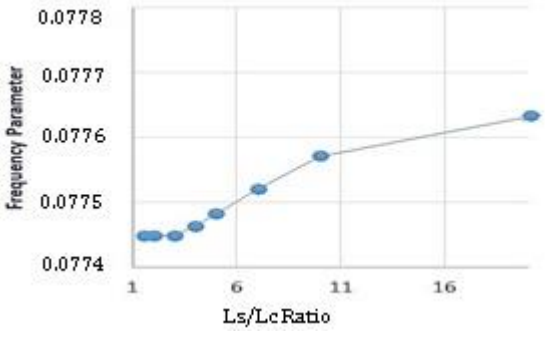


(d)

**Fig. 7**. Effect of length ratio of shell on natural frequency for $n$=5, a) $\frac{L_s}{R_s} = \mathbf{0.5}$, b) $\frac{L_s}{R_s} = \mathbf{1}$, c) $\frac{L_s}{R_s} = \mathbf{2}$, and d) $\frac{L_s}{R_s} = \mathbf{3}$

As can be seen, regardless of the value of $\frac{L_S}{R_S}$ ratio, the natural frequency is increased by increasing the value of $\frac{L_S}{L_C}$.

## 13. Effect of the Orthotropic Ratio

Fig. 8 presents the variation of the frequency parameter versus the orthotropic ratio $(E_1/E_2)$ studied for different lay-ups.

Based on the obtained results, the natural frequency of the shell is decreased by increasing the ratio of $E_1/E_2$. For higher ratios of $E_1/E_2$, the rate of decreasing natural frequency is decreased. Moreover, it is observed that the lay-ups [0/90 / 0 / 90] and [0/45 / 0 / 45] have the greatest and smallest natural frequencies, respectively.

## 14. Effect of Number of Layers

In this section, the effect of the number of layers $(N_L)$ on the natural frequency is investigated. Figs. 9 to 12 show the effect of changing the number of layers for a constant thickness and lay-up $[0/90]_n$ and its effect on the natural frequency.

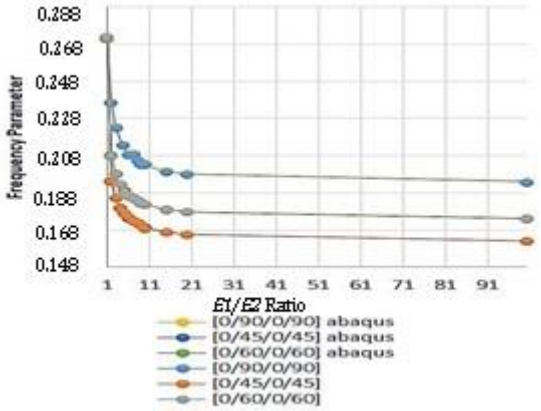


**Fig. 8**. Effect of elasticity modulus on the natural frequency ($n$=5)

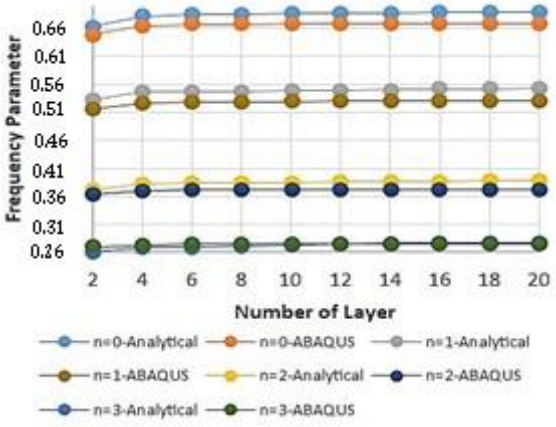


**Fig. 9**. Effect of number of layers for a constant thickness and lay-up $[\mathbf{0/90}]_n$ on the natural frequency at circumferential wave numbers $n$=0 to $n$=3

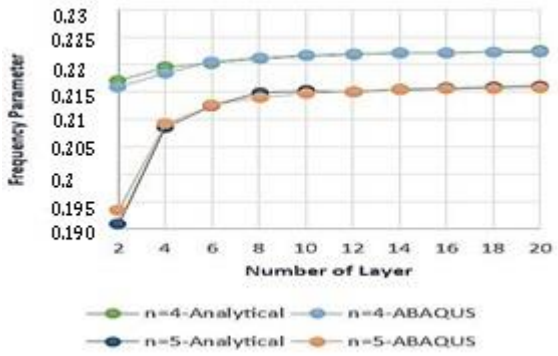


**Fig. 10**. Effect of number of layers for a constant thickness and lay-up $[\mathbf{0/90}]_n$ on the natural frequency at $n$ = 4 to 5

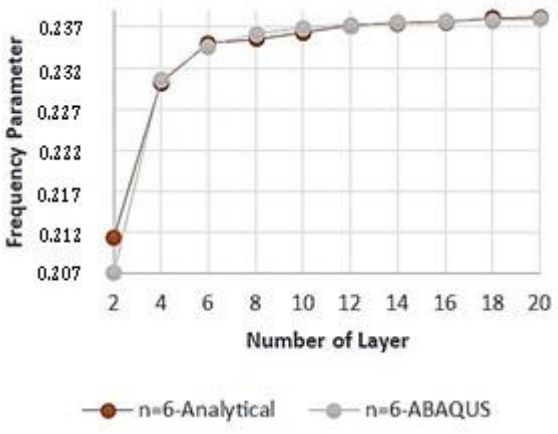


**Fig. 11**. Effect of number of layers for a constant thickness and lay-up $[\mathbf{0/90}]_n$ on the natural frequency at $n$ = 6

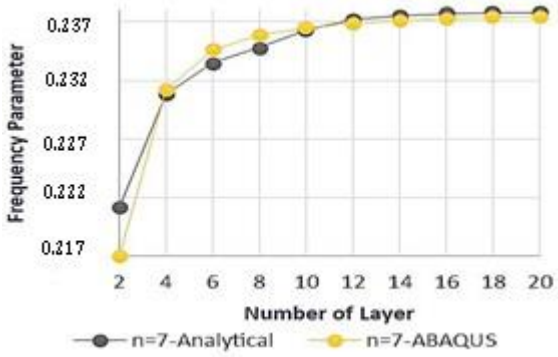


**Fig. 12**. Effect of number of layers for a constant thickness and lay-up $[\mathbf{0/90}]_n$ on the natural frequency at $n$=7

As can be seen in these figures, the natural frequency of the shell is increased by increasing the number of layers in a constant thickness. The rate of increase is very much greater at lower values of the number of layers. The maximum percentage discrepancy between the numerical and analytical results is 4%, which occurs in Fig. 9 at $N_L = 20$ and $n$=1.

## 15. Effect of Internal pressure

The effect of internal pressure on the natural frequency is studied as shown in Table 6.

**Table 6.** Effect of internal pressure on the frequency parameter of a conical-cylindrical composite shell

| $P$(Pa) | $\omega_c$ |
|---|---|
| 0 | 0.1910 |
| 1 | 0.1910 |
| 10 | 0.1910 |
| $10^2$ | 0.1910 |
| $10^3$ | 0.1912 |
| $10^4$ | 0.1930 |
| $10^5$ | 0.2125 |
| $10^6$ | 0.3381 |
| $10^7$ | 0.9265 |
| $10^8$ | 2.2111 |

As shown in Table 6, by increasing the internal pressure, the natural frequency is increased as well. Although the natural frequency is not affected considerably by lower values of $P$, for higher values of $P$, it increases dramatically.

## 16. Effect Axial Compressive Force

The effect of axial compressive force on natural frequency is studied in Table 7.

Based on the obtained results, by increasing the axial compressive force, the natural frequency is decreased and reaches 0 at a specific load (buckling load).

## 17. Effect of Fiber Angle

To study the effect of fiber angle on the natural frequencies, a composite shell with lay-up $[\pm\emptyset]$ was considered. The results are shown in Fig. 13.

**Table 7**. Effect of axial compressive force on the frequency parameter of a conical-cylindrical composite shell

| Na*2*pi*R(N) | $\omega_c$ |
|---|---|
| 0 | 0.1910 |
| 10 | 0.1908 |
| 100 | 0.1898 |
| 1000 | 0.1789 |
| 2000 | 0.1623 |
| 3000 | 0.1426 |
| 4000 | 0.1013 |
| 5000 | 0 |

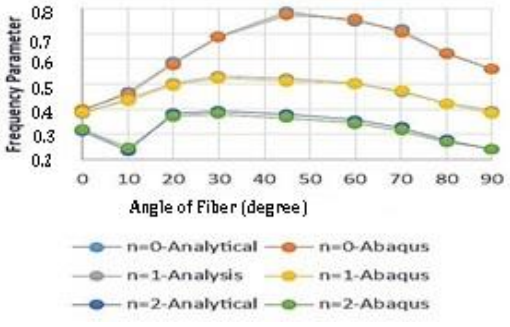


**Fig. 13**. Effect of fiber angle of the composite shell with lay-up $[\pm\emptyset]$ on the natural frequency

As can be seen, in each circumferential wave number ($n$), the behavior of natural frequency is changed by changing the fiber angle.

In axisymmetric mode ($n$=0), by increasing the angle of the fiber, the natural frequency is increased up to the fiber angle $\emptyset = 45°$. Beyond $\emptyset = 45°$, the natural frequency is decreased. The minimum frequency occurs at $\emptyset = 0°$. For $n$=1, by increasing the angle of the fiber, the natural frequency is increased up to the fiber angle of $\emptyset$=30°. Beyond $\emptyset$=30°, the natural frequency is decreased. Naturally, the slope of decreasing frequency is increased for fiber angles between $\emptyset = 60°$ and $\emptyset = 90°$. The minimum frequency occurs at $\emptyset = 0°$ and $\emptyset = 90°$.

At $n$=2, by increasing the angle of the fiber, the natural frequency is decreased strongly between $\emptyset = 0°$ and $\emptyset = 10°$. From $\emptyset$=10° to $\emptyset$=20°, the natural frequency is increased and then decreased. The minimum frequency occurs at $\emptyset = 10°$ and the maximum value of it occurs at $\emptyset = 30°$.

## 18. Effect of Orthotropic Ratio

In this section, the effect of orthotropic ratio and fiber angle on the natural frequency of the single-layer composite is studied. Fig. 13 presents the variation of the natural frequency correspondent to the axisymmetric mode ($n$=0) versus fiber angle for a single-layered composite combined shell for different orthotropic ratios.

As shown in Fig. 14, for lower orthotropic ratios, the change in the natural frequency caused by varying the angle of the fiber is negligible. For $E_1/E_2 = 1$, the natural frequency is first increased up to 45° at which the maximum occurs. For $E_1/E_2 = 2$, the maximum occurs at 60°. For orthotropic ratios equal to 3:10, this maximum occurs at a fiber angle of 70°. As the orthotropic ratio increases, the natural frequency is decreased. Regardless of the value of the orthotropic ratio, by increasing the fiber angle, the natural frequency is first increased and then decreased.

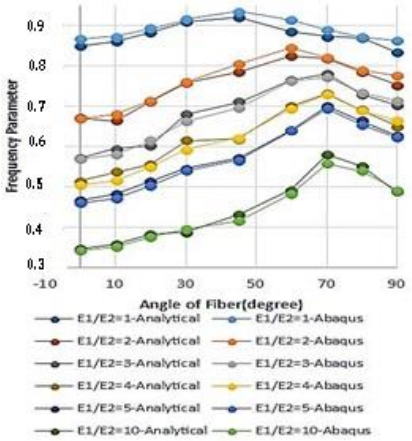


**Fig. 14**. The natural frequency of combined shell with single layer versus angle of fiber for various orthotropic ratios ($n$=0)

## 19. Conclusion

In the present study, a new approach is introduced to obtain the free vibrational characteristics of combined composite cylindrical-conical shells. In the previous studies, the present problem was solved using classical shell theories but the effect of shear deformation was not taken into account. This approach contains the effect of first-order shear deformation in the shell theory. Moreover, the effect of geometric and material parameters on the natural frequency is investigated and the effect of pre-load of internal pressure and an axial compressive force is studied. The results showed that the fiber angle and orthotropic ratio affect the frequency behavior of joined conical-cylindrical shells. It shows that for lower orthotropic ratios, the change ub the natural frequency by varying the angle of the fiber is negligible. Furthermore, the natural frequency of the shell is increased by increasing the number of layers in a constant thickness. The natural frequency of the shell is decreased by increasing the ratio of $E_1/E_2$. For higher ratios of $E_1/E_2$, the rate of decreasing natural frequency is decreased. Finally, by increasing the semi-vertex angle of the cone, the natural frequency is converged to an almost constant value for higher values of the circumferential wave number.
Results are verified by making a comparison with the literature and the results obtain using ABAQUS. Good agreement is observed.

## References

[1] Irie, "Natural Frequencies of Truncated Conical Shells," Journal of Sound and Vibration, vol. 92, pp. 447-453, 1984 .

[2] L. Tong, "Free Vibration of Orthotropic Conical Shells," International Journal Engng Science, vol. 31, no. Pergamon Press Ltd, pp. 719-733, 1993 .

[3] L. Tong, "Free Vibration of Laminated Conical Shells Including Transverse Shear Deformation," International Journal of Solid Mechanics, vol. 31, pp. 443-456, 1994 .

[4] D. He, D. Shi, Q. Wang, Ch. Ma, "A unified power series method for vibration analysis of composite laminate conical, cylindrical shell and annular plate", Structures, Vol. 29, pp. 305-327, 2021.

[5] M. Kouchakzadeh and M. Shakouri, "Free vibration analysis of joined cross-ply laminated conical shells," International Journal of Mechanical Sciences, vol. 78, pp. 118-125, 2014 .

[6] Mauro Caresta and Nicole J. Kessissoglou, "Free vibrational characteristics of isotropic coupled cylindrical-conical shells," Journal

of Sound and Vibration, vol. 329, pp. 733-751, 2010 .

[7] M. Xianglong, J. Guoyong, X. Yeping and L. Zhigang, "Free and forced vibration analysis of coupled conical–cylindrical shells with arbitrary boundary conditions," International Journal of Mechanical Sciences, vol. 88, pp. 122-137, 2014 .

[8] H. Bagheria, Y. Kiani and M. Eslami, "Free vibration of joined conical-conical shells," Thin-Walled Structures, vol. 120, p. 446–457, 2017 .

[9] Sh. Mohammadrezazadeh and A. Jafari, Nonlinear vibration analysis of laminated composite angle-ply cylindrical and conical shells, Composite Structures, vol. 255, 2021,112867.

[10] B. Qin, R. Zhong, T. Wang, Q. Wang, Y. Xu, Z. Hu, A unified Fourier series solution for vibration analysis of FG-CNTRC cylindrical, conical shells and annular plates with arbitrary boundary conditions, Composite Structures, vol. 232, 2020, 111549.

[11] E. Efraim and M. Eisenberger, "Exact vibration frequencies of segmented axisymmetric shells," Thin-Walled Structure, vol. 44, pp. 281-289, 2006 .

[12] H. Garnet and J. Kempner, "Axisymmetric Free Vibrations of Conical Shells," Journal of Applied Mechanics, no. ASME, 1964 .

[13] J. Reddy, Mechanics of Laminated Composite Plate and Shell, Theory and Analysis, United States of America: CRC PRESS, 2003 .

[14] ASM HANDBOOK - Composites, vol. 21, ASM International, Dec.2001 .

[15] G. Lubin, Handbook of composites, New York: Van Nostrand Reinhold, 1982 .

## Appendix

$$T_{11} = k_3 G_{11} - k_2 G_{41} \quad \text{A-1}$$

$$T_{12} = k_3 G_{12} - k_2 G_{42} \quad \text{A-2}$$

$$T_{13} = k_3 G_{13} - k_2 G_{43} \quad \text{A-3}$$

$$T_{14} = k_3 G_{14} - k_2 G_{44} \quad \text{A-4}$$

$$T_{15} = k_3 G_{15} - k_2 G_{45} \quad \text{A-5}$$

$$T_{16} = k_3 G_{16} - k_2 G_{46} \quad \text{A-6}$$

$$T_{17} = k_3 G_{17} - k_2 G_{47} \quad \text{A-7}$$

$$T_{18} = k_3 G_{18} - k_2 G_{48} \quad \text{A-8}$$

$$T_{19} = k_3 G_{19} - k_2 G_{49} \quad \text{A-9}$$

$$T_{1,10} = k_3 G_{1,10} - k_2 G_{4,10} \quad \text{A-10}$$

$$T_{1,11} = k_3 G_{1,11} - k_2 G_{4,11} \quad \text{A-11}$$

$$T_{1,12} = k_3 G_{1,12} - k_2 G_{4,12} \quad \text{A-12}$$

$$T_{1,13} = k_3 G_{1,13} - k_2 G_{4,13} \quad \text{A-13}$$

$$T_{1,14} = k_3 G_{1,14} - k_2 G_{4,14} \quad \text{A-14}$$

$$T_{1,15} = k_3 G_{1,15} - k_2 G_{4,15} \quad \text{A-15}$$

$$T_{21} = \lambda_3 G_{21} - \lambda_2 G_{51} \quad \text{A-16}$$

$$T_{22} = \lambda_3 G_{22} - \lambda_2 G_{52} \quad \text{A-17}$$

$$T_{23} = \lambda_3 G_{23} - \lambda_2 G_{53} \quad \text{A-18}$$

$$T_{24} = \lambda_3 G_{24} - \lambda_2 G_{54} \quad \text{A-19}$$

$$T_{25} = \lambda_3 G_{25} - \lambda_2 G_{55} \quad \text{A-20}$$

$$T_{26} = \lambda_3 G_{26} - \lambda_2 G_{56} \quad \text{A-21}$$

$$T_{27} = \lambda_3 G_{27} - \lambda_2 G_{57} \quad \text{A-22}$$

$$T_{28} = \lambda_3 G_{28} - \lambda_2 G_{58} \quad \text{A-23}$$

$$T_{29} = \lambda_3 G_{29} - \lambda_2 G_{59} \quad \text{A-24}$$

$$T_{2,10} = \lambda_3 G_{2,10} - \lambda_2 G_{5,10} \quad \text{A-25}$$

$$T_{2,11} = \lambda_3 G_{2,11} - \lambda_2 G_{5,11} \quad \text{A-26}$$

$$T_{2,12} = \lambda_3 G_{2,12} - \lambda_2 G_{5,12} \quad \text{A-27}$$

$$T_{2,13} = \lambda_3 G_{2,13} - \lambda_2 G_{5,13} \quad \text{A-28}$$

$$T_{2,14} = \lambda_3 G_{2,14} - \lambda_2 G_{5,14} \quad \text{A-29}$$

$$T_{3,i} = \frac{G_{3,i}}{(A_{55} + N_a)} \quad (i = 1,2,3, \dots \dots ,21,22) \quad \text{A-30}$$

$$T_{41} = -k_2 G_{11} + k_1 G_{41} \quad \text{A-31}$$

$$T_{42} = -k_2 G_{12} + k_1 G_{42} \quad \text{A-32}$$

$$T_{43} = -k_2 G_{13} + k_1 G_{43} \quad \text{A-33}$$

$$T_{44} = -k_2 G_{14} + k_1 G_{44} \quad \text{A-34}$$

$$T_{45} = -k_2 G_{15} + k_1 G_{45} \quad \text{A-35}$$

$$T_{46} = -k_2 G_{16} + k_1 G_{46} \quad \text{A-36}$$

$$T_{47} = -k_2 G_{17} + k_1 G_{47} \quad \text{A-37}$$

$$T_{48} = -k_2 G_{18} + k_1 G_{48} \quad \text{A-38}$$

$$T_{49} = -k_2 G_{19} + k_1 G_{49} \quad \text{A-39}$$

$$T_{4,10} = -k_2 G_{1,10} + k_1 G_{4,10} \quad \text{A-40}$$

$$T_{4,11} = -k_2 G_{1,11} + k_1 G_{4,11} \quad \text{A-41}$$

$$T_{4,12} = -k_2 G_{1,12} + k_1 G_{4,12} \quad \text{A-42}$$

$$T_{4,13} = -k_2 G_{1,13} + k_1 G_{4,13} \quad \text{A-43}$$

$$T_{4,14} = -k_2 G_{1,14} + k_1 G_{4,14} \quad \text{A-44}$$

$$T_{4,15} = -k_2 G_{1,15} + k_1 G_{4,15} \quad \text{A-45}$$

$$T_{51} = -\lambda_2 G_{21} + \lambda_1 G_{51} \quad \text{A-46}$$

$$T_{52} = -\lambda_2 G_{22} + \lambda_1 G_{52} \quad \text{A-47}$$

$$T_{53} = -\lambda_2 G_{23} + \lambda_1 G_{53} \quad \text{A-48}$$

$$T_{54} = -\lambda_2 G_{24} + \lambda_1 G_{54} \quad \text{A-49}$$

$$T_{55} = -\lambda_2 G_{25} + \lambda_1 G_{55} \quad \text{A-50}$$

$$T_{56} = -\lambda_2 G_{26} + \lambda_1 G_{56} \quad \text{A-51}$$

$$T_{57} = -\lambda_2 G_{27} + \lambda_1 G_{57} \quad \text{A-52}$$

$$T_{58} = -\lambda_2 G_{28} + \lambda_1 G_{58} \quad \text{A-53}$$

$$T_{59} = -\lambda_2 G_{29} + \lambda_1 G_{59} \quad \text{A-54}$$

$$T_{5,10} = -\lambda_2 G_{2,10} + \lambda_1 G_{5,10} \quad \text{A-55}$$

$$T_{5,11} = -\lambda_2 G_{2,11} + \lambda_1 G_{5,11} \quad \text{A-56}$$

$$T_{5,12} = -\lambda_2 G_{2,12} + \lambda_1 G_{5,12} \quad \text{A-57}$$

$$T_{5,13} = -\lambda_2 G_{2,13} + \lambda_1 G_{5,13} \quad \text{A-58}$$

$$T_{5,14} = -\lambda_2 G_{2,14} + \lambda_1 G_{5,14} \quad \text{A-59}$$

where:

$$k_0 = A_{11} D_{11} - B_{11}^2 \quad \text{A-60}$$

$$k_1 = \frac{A_{11}}{k_0} \quad \text{A-61}$$

$$k_2 = \frac{B_{11}}{k_0} \quad \text{A-62}$$

$$k_3 = \frac{D_{11}}{k_0} \quad \text{A-63}$$

$$\lambda_0 = A_{66} D_{66} - B_{66}^2 \quad \text{A-64}$$

$$\lambda_1 = \frac{A_{66}}{\lambda_0} \quad \text{A-65}$$

$$\lambda_2 = \frac{B_{66}}{\lambda_0} \quad \text{A-66}$$

$$\lambda_3 = \frac{D_{66}}{\lambda_0} \quad \text{A-67}$$

$$G_{11} = -\frac{A_{11}(2m+1)sin\,\alpha}{R_0(m+2)} \quad \text{A-68}$$

$$G_{12} = -\frac{(m^2 A_{11} - A_{22})sin^2\alpha - n^2 A_{66}}{R_0^2(m+2)(m+1)} - \frac{I_0\omega^2}{(m+2)(m+1)} \quad \text{A-69}$$

$$G_{13} = -\frac{2I_0\omega^2 sin\alpha}{R_0(m+2)(m+1)} \quad \text{A-70}$$

$$G_{14} = -\frac{I_0\omega^2 sin^2\alpha}{R_0{}^2(m+2)(m+1)} \quad \text{A-71}$$

$$G_{15} = -\frac{A_{126}n}{R_0(m+2)} \quad \text{A-72}$$

$$G_{16} = \frac{(-mA_{126} + A_{226})nsin\alpha}{R_0^2(m+2)(m+1)} \quad \text{A-73}$$

$$G_{17} = -\frac{A_{12}cos\,\alpha}{R_0(m+2)} \quad \text{A-74}$$

$$G_{18} = \frac{(-mA_{12} + A_{22})\,sin\alpha\,cos\alpha}{R_0^2(m+2)(m+1)} \quad \text{A-75}$$

$$G_{19} = 0 \quad \text{A-76}$$

$$G_{1,10} = -\frac{B_{11}(2m+1)sin\,\alpha}{R_0(m+2)} \quad \text{A-77}$$

$$G_{1,11} = -\frac{(m^2 B_{11} - B_{22})sin^2\alpha}{R_0^2(m+2)(m+1)} \quad \text{A-78}$$

$$G_{1,12} = 0 \quad \text{A-79}$$

$$G_{1,13} = 0 \quad \text{A-80}$$

$$G_{1,14} = -\frac{B_{126}n}{R_0(m+2)} \quad \text{A-81}$$

$$G_{1,15} = \frac{(-mB_{126} + B_{226})nsin\alpha}{R_0^2(m+2)(m+1)} \quad \text{A-82}$$

$$G_{21} = \frac{A_{126}n}{R_0(m+2)} \quad \text{A-83}$$

$$G_{22} = \frac{(mA_{126} + A_{226})nsin\alpha}{R_0^2(m+2)(m+1)} \quad \text{A-84}$$

$$G_{23} = -\frac{A_{66}(2m+1)sin\,\alpha}{R_0(m+2)} \quad \text{A-85}$$

$$G_{24} = -\frac{A_{66}(m^2-1)sin^2\alpha - n^2 A_{22} - A_{44}cos}{R_0^2(m+2)(m+1)} - \frac{I_0\omega^2}{(m+2)(m+1)} \quad \text{A-86}$$

$$G_{25} = -\frac{2I_0\omega^2 sin\alpha}{R_0(m+2)(m+1)} \quad \text{A-87}$$

$$G_{26} = -\frac{I_0\omega^2 sin^2\alpha}{R_0{}^2(m+2)(m+1)} \quad \text{A-88}$$

$$G_{27} = \frac{(A_{22} + A_{44})n\,cos\alpha}{R_0^2(m+2)(m+1)} \quad \text{A-89}$$

$$G_{28} = 0 \quad \text{A-90}$$

$$G_{29} = \frac{B_{126}n}{R_0(m+2)} \quad \text{A-91}$$

$$G_{2,10} = \frac{(mB_{126} + B_{226})nsin\alpha}{R_0^2(m+2)(m+1)} \quad \text{A-92}$$

$$G_{2,11} = -\frac{B_{66}(2m+1)sin\,\alpha}{R_0(m+2)} \quad \text{A-93}$$

$$G_{2,12} = -\frac{B_{66}(m^2-1)sin^2\alpha - n^2 B_{22} - A_{44}cos}{R_0^2(m+2)(m+1)} \quad \text{A-94}$$

$$G_{2,13} = \frac{A_{44}cos\alpha}{A_{66}R_0^2(m+2)(m+1)} \quad \text{A-95}$$

$$G_{2,14} = 0 \quad \text{A-96}$$

$$G_{31} = \frac{A_{12}cos\,\alpha}{R_0(m+2)} \quad \text{A-97}$$

$$G_{32} = \frac{(mA_{12} + A_{22})\, sin\alpha\, cos\, \alpha}{R_0^2(m+2)(m+1)} \quad \text{A-98}$$

$$G_{33} = \frac{(A_{22} + A_{44})n\, cos\alpha}{R_0^2(m+2)(m+1)} \quad \text{A-99}$$

$$G_{34} = -\frac{A_{55}(2m+1)sin\, \alpha}{R_0(m+2)} \quad \text{A-100}$$

$$G_{35} = -\frac{A_{55}m^2sin^2\alpha - n^2A_{44} - A_{22}cos^2\alpha}{R_0^2(m+2)(m+1)} - \frac{I_0\omega^2}{(m+2)(m+1)} \quad \text{A-101}$$

$$G_{3,6} = -\frac{2I_0\omega^2 sin\alpha}{R_0(m+2)(m+1)} \quad \text{A-102}$$

$$G_{3,7} = -\frac{I_0\omega^2 sin^2\alpha}{R_0(m+2)(m+1)} \quad \text{A-103}$$

$$G_{3,8} = -\frac{B_{12}\, cos\, \alpha - A_{55}R_0}{R_0(m+2)} \quad \text{A-104}$$

$$G_{3,9} = -\frac{A_{55}R_0(1+2m)\, sin\, \alpha - (B_{12}m + B_{22})}{R_0^2(m+2)(m+1)} \quad \text{A-105}$$

$$G_{3,10} = -\frac{A_{55}m\, sin^2\alpha}{R_0^2(m+2)(m+1)} \quad \text{A-106}$$

$$G_{3,11} = \frac{(B_{22}\, cos\, \alpha - A_{44}R_0)n}{R_0^2(m+2)(m+1)} \quad \text{A-107}$$

$$G_{3,12} = -\frac{A_{44}\, n\, sin\, \alpha}{R_0^2(m+2)(m+1)} \quad \text{A-108}$$

$$G_{41} = -\frac{B_{11}(2m+1)sin\, \alpha}{R_0(m+2)} \quad \text{A-109}$$

$$G_{42} = -\frac{(m^2B_{11} - B_{22})sin^2\alpha - n^2B_{66}}{R_0^2(m+2)(m+1)} \quad \text{A-110}$$

$$G_{4,3} = 0 \quad \text{A-111}$$

$$G_{4,4} = 0 \quad \text{A-112}$$

$$G_{45} = -\frac{B_{126}n}{R_0\,(m+2)} \quad \text{A-113}$$

$$G_{46} = \frac{(-mB_{126} + B_{226})nsin\alpha}{R_0^2(m+2)(m+1)} \quad \text{A-114}$$

$$G_{47} = -\frac{B_{12}cos\, \alpha - A_{55}R_0}{R_0(m+2)} \quad \text{A-115}$$

$$G_{48} = -\frac{(mB_{12} - B_{22})cos\alpha sin\alpha - 2A_{55}R_0 m sin\alpha}{R_0^2(m+2)(m+1)} \quad \text{A-116}$$

$$G_{49} = \frac{A_{55}(m-1)\, sin^2\, \alpha}{{R_0}^2\,(m+2)(m+1)} \quad \text{A-117}$$

$$G_{4,10} = -\frac{D_{11}(2m+1)sin\, \alpha}{R_0(m+2)} \quad \text{A-118}$$

$$G_{4,11} = -\frac{(m^2D_{11} - D_{22})sin^2\alpha - n^2D_{66} - A_{55}{R_0}^2}{R_0^2(m+2)(m+1)} - \frac{I_2\omega^2}{(m+2)(m+1)} \quad \text{A-119}$$

$$G_{4,12} = \frac{2(A_{55} - I_2\omega^2)sin\, \alpha}{R_0(m+2)(m+1)} \quad \text{A-120}$$

$$G_{4,13} = \frac{(A_{55} - I_2\omega^2)sin^2\, \alpha}{{R_0}^2(m+2)(m+1)} \quad \text{A-121}$$

$$G_{4,14} = -\frac{D_{126}n}{R_0\,(m+2)} \quad \text{A-122}$$

$$G_{4,15} = \frac{(-mD_{126} + D_{226})nsin\alpha}{R_0^2(m+2)(m+1)} \quad \text{A-123}$$

$$G_{51} = \frac{B_{126}n}{R_0\,(m+2)} \quad \text{A-124}$$

$$G_{52} = \frac{(mB_{126} + B_{226})nsin\alpha}{R_0^2(m+2)(m+1)} \quad \text{A-125}$$

$$G_{53} = -\frac{B_{66}(2m+1)sin\, \alpha}{R_0(m+2)} \quad \text{A-126}$$

$$G_{54} = -\frac{B_{66}(m^2-1)sin^2\alpha - n^2B_{22} + A_{44}\, R_0 cos\, \alpha}{R_0^2(m+2)(m+1)} \quad \text{A-127}$$

$$G_{55} = -\frac{A_{44}\, sin\alpha\, cos\, \alpha}{R_0^2(m+2)(m+1)} \quad \text{A-128}$$

$$G_{56} = 0 \quad \text{A-129}$$

$$G_{57} = \frac{(B_{22}cos\alpha - R_0A_{44})n}{R_0^2(m+2)(m+1)} \quad \text{A-130}$$

$$G_{58} = -\frac{nA_{44}\, sin\alpha}{R_0^2(m+2)(m+1)} \quad \text{A-131}$$

$$G_{59} = \frac{D_{126}n}{R_0\,(m+2)} \quad \text{A-132}$$

$$G_{5,10} = \frac{(mD_{126} + D_{226})nsin\alpha}{R_0^2(m+2)(m+1)} \quad \text{A-133}$$

$$G_{5,11} = -\frac{D_{66}(2m+1)sin\, \alpha}{R_0(m+2)} \quad \text{A-134}$$

$$G_{5,12} = -\frac{D_{66}(m^2-1)sin^2\alpha - n^2D_{22} - A_{44}R_0^2}{R_0^2(m+2)(m+1)} - \frac{I_2\omega^2}{(m+2)(m+1)} \quad \text{A-135}$$

$$G_{5,13} = \frac{2(A_{44} - I_2\omega^2)sin\, \alpha}{R_0(m+2)(m+1)} \quad \text{A-136}$$

$$G_{5,14} = \frac{(A_{44} - I_2\omega^2)sin^2\, \alpha}{{R_0}^2(m+2)(m+1)} \quad \text{A-137}$$

where:

$$A_{126} = A_{12} + A_{66} \quad \text{A-138}$$

$$A_{226} = A_{22} + A_{66} \quad \text{A-139}$$

$$D_{126} = D_{12} + D_{66} \quad \text{A-140}$$

$$D_{226} = D_{22} + D_{66} \quad \text{A-141}$$

$$B_{126} = B_{12} + B_{66} \quad \text{A-142}$$

$$B_{226} = B_{22} + B_{66} \quad \text{A-143}$$

A-144

$$\begin{aligned} a_{m+2} = {} & T_{11}a_{m+1} + T_{12}a_m + T_{13}a_{m-1} + T_{14}a_{m-2} \\ & + T_{15}b_{m+1} + T_{16}b_m + T_{17}c_{m+1} \\ & + T_{1,8}c_m + T_{1,9}c_{m-1} + T_{1,10}d_{m+1} \\ & + T_{1,11}d_m + T_{1,12}d_{m-1} \\ & + T_{1,13}d_{m-2} + T_{1,14}f_{m+1} \\ & + T_{1,15}f_m \end{aligned}$$

A-145

$$\begin{aligned} & b_{m+2} \\ & = T_{21}a_{m+1} + T_{22}a_m + T_{23}b_{m+1} + T_{24}b_m \\ & + T_{25}b_{m-1} + T_{26}b_{m-2} + T_{2,7}c_m + T_{2,8}c_{m-1} \\ & + T_{2,9}d_{m+1} + T_{2,10}d_m + T_{2,11}f_{m+1} + T_{2,12}f_m + T_{2,13}f_{m-1} \\ & + T_{2,14}f_{m-2} \end{aligned}$$

A-146

$$\begin{aligned} c_{m+2} = {} & T_{31}a_{m+1} + T_{32}a_m + T_{33}b_m + T_{34}c_{m+1} \\ & + T_{3,5}c_m + T_{3,6}c_{m-1} + T_{3,7}c_{m-2} \\ & + T_{3,8}d_{m+1} + T_{3,9}d_m \\ & + T_{3,10}d_{m-1} + T_{3,11}f_m \\ & + T_{3,12}f_{m-1} \end{aligned}$$

A-147

$$\begin{aligned} d_{m+2} = {} & T_{41}a_{m+1} + T_{42}a_m + T_{43}a_{m-1} + T_{44}a_{m-2} \\ & + T_{45}b_{m+1} + T_{46}b_m + T_{47}c_{m+1} \\ & + T_{4,8}c_m + T_{4,9}c_{m-1} + T_{4,10}d_{m+1} \\ & + T_{4,11}d_m + T_{4,12}d_{m-1} \\ & + T_{4,13}d_{m-2} + T_{4,14}f_{m+1} \\ & + T_{4,15}f_m \end{aligned}$$

A-148

$$\begin{aligned} f_{m+2} = {} & T_{51}a_{m+1} + T_{52}a_m + T_{53}b_{m+1} + T_{54}b_m \\ & + T_{55}b_{m-1} + T_{56}b_{m-2} + T_{5,7}c_m \\ & + T_{5,8}c_{m-1} + T_{5,9}d_{m+1} \\ & + T_{5,10}d_m + T_{5,11}f_{m+1} + T_{5,12}f_m \\ & + T_{5,13}f_{m-1} + T_{5,14}f_{m-2} \end{aligned}$$